

The plasma soluble CSF1R level is a promising prognostic indicator for pediatric Langerhans cell histiocytosis

Zhigang Li¹, Ting Zhu¹, Chanjuan Wang¹, Hong-Yun Lian¹, Hong-Hao Ma¹, Dong Wang¹, Tianyou Wang¹, rui zhang¹, and Lei Cui¹

¹Beijing Children's Hospital Capital Medical University

April 05, 2024

Abstract

Langerhans cell histiocytosis (LCH) is a rare hematologic neoplasm characterized by the clonal proliferation of Langerhans-like cells. Colony-stimulating Factor 1 receptor (CSF1R) is a membrane-bound receptor that is highly expressed in LCH cells and tumor-associated macrophages. In this study, a soluble form of CSF1R protein (sCSF1R) was identified by plasma proteome profiling, and its role in evaluating LCH prognosis was explored. We prospectively measured plasma sCSF1R levels in 104 LCH patients and 10 healthy children using ELISA. Plasma sCSF1R levels were greater in LCH patients than in healthy controls ($P < 0.001$) and significantly differed among the three disease extents, with the highest level in MS RO+ LCH patients ($P < 0.001$). Accordingly, immunofluorescence showed the highest level of membrane-bound CSF1R in MS RO+ patients. Furthermore, the plasma sCSF1R concentration at diagnosis could efficiently predict the prognosis of LCH patients treated with standard first-line treatment (AUC = 0.782, $P < 0.001$). Notably, dynamic monitoring of sCSF1R levels could predict relapse early in patients receiving BRAF inhibitor treatment. In vitro drug sensitivity data showed that sCSF1R increased resistance to Ara-C in THP-1 cells expressing ectopic *BRAF*-V600E. Overall, the plasma sCSF1R level at diagnosis and during follow-up is of great clinical importance in pediatric LCH patients.

Introduction

Langerhans cell histiocytosis (LCH) is a rare hematologic neoplasm characterized by the accumulation of CD1a⁺ CD207⁺ histiocytes and inflammatory infiltrates^{1,2}. This disease most commonly affects children with highly variable clinical manifestations, ranging from a single self-limited bone or skin lesion to life-threatening disseminated disease^{1,2}. The mechanisms of pathogenesis are underpinned by alterations in the MAPK pathway, with 50% to 60% of patients exhibiting the *BRAF*-V600E mutation in lesions¹. Although stratified treatment strategies have improved the overall survival (OS) rate of pediatric LCH patients in recent decades and BRAF or MEK inhibitors have shown good short-term effectiveness and tolerability in recurrent/refractory LCH, relapse has remained the major cause of treatment failure³. Therefore, there is a pressing need to identify effective prognostic factors to predict recurrence and refine risk stratification for LCH patients.

Colony-stimulating Factor 1 receptor (CSF1R) is a transmembrane protein that functions as a cell membrane receptor^{4,5}; it binds ligands through its ectodomain to activate intercellular signaling pathways, which control innate immune responses⁵. CSF1R is a helpful marker for distinguishing florid dermatopathic lymphadenopathy from Langerhans cell neoplasms⁶. High expression of CSF1R in LCH cells and tumor-associated macrophages (TAMs) from LCH patients further supports the importance of CSF1R in LCH disease⁷. Intriguingly, a soluble form of CSF1R (sCSF1R), a truncated CSF1R protein, has been reported in goldfish serum⁸. sCSF1R lacks the transmembrane and intracellular domains but retains the ligand-binding region. However, whether sCSF1R is generated through alternative splicing or proteolytic cleavage of the extracellular domain of the full-length receptor is not fully understood⁸. A peptide derived

from CSF1R has been identified in human cerebrospinal fluid (CSF) as a potential biomarker for Parkinson's disease compared to healthy controls⁹. However, whether sCSF1R can be detected in the plasma of LCH patients as a biomarker must be explored.

This study is the first to identify sCSF1R as a robust plasma biomarker by plasma proteome profiling. We further detected plasma sCSF1R levels at diagnosis and during follow-up with an immunoassay ELISA to investigate its prognostic value. Finally, we explored the effect of sCSF1R on chemotherapeutic drug sensitivity at the cellular level.

Patients and Methods

Patients

A total of 139 consecutive pediatric patients with newly diagnosed LCH were admitted to our hospital between January 1, 2020, and June 30, 2021. One hundred and fourteen patients with available plasma samples were prospectively enrolled in the present study cohort. Twenty-five patients were excluded due to loss to follow-up after diagnosis ($n = 18$) or lack of plasma samples ($n = 7$). This study was approved by the Beijing Children's Hospital Ethics Committee and was conducted in accordance with the Declaration of Helsinki. Informed consent was obtained from the guardians of the patients.

Diagnosis and therapeutic regimen

Histopathological examination confirmed that the patients had LCH, as indicated by positive immunostaining for CD1a and Langerin (CD207) in the lesion tissues. Patients were divided into single-system (SS) or multisystem (MS) LCH according to the number of organs or systems involved and classified as risk organ (RO) positive (liver, spleen, and/or hematological system) or negative according to the extent of LCH^[1].

Patients were treated with a systemic chemotherapy regimen (CCHG-LCH 2019 protocol, www.chictr.org.cn, identifier: ChiCTR1900025783), which was based on the LCH III and LCH-S-2005 protocols¹⁰. Briefly, the first-line treatment was vindesine-steroid combination therapy, beginning with one or two six-week courses of intensive initial induction therapy followed by maintenance therapy. The BRAF inhibitor dabrafenib was given to patients who carried the *BRAF* -V600E mutation and had recurrent/refractory LCH disease. The details of the treatment are shown in the Supplementary Methods.

Mass spectrometry-based plasma proteomics analysis

We collected diagnostic plasma samples from 11 patients, including 5 with MS RO+, 6 with SS-LCH and 5 healthy controls, for proteomic analysis (Supplementary Table S1). Date-independent acquisition (DIA) combined with liquid chromatography–tandem mass spectrometry (LC–MS/MS) analysis was performed. The differentially expressed proteins (DEPs) between MS RO+ LCH and SS LCH were explored. Gene Ontology (GO) and Kyoto Encyclopedia of Genes and Genomes (KEGG) enrichment analyses were also conducted to reveal the functions of the DEPs in biological processes.

Single-cell RNA-seq (scRNA) analysis

We performed a bioinformatics analysis using a single-cell RNA sequencing (scRNA-seq) dataset of PBMCs from our previous study¹¹. Briefly, we divided the samples into two groups: the MS RO+ LCH group ($n = 7$) and the SS LCH group ($n = 3$). Differentially expressed genes (DEGs) were also analyzed.

ELISA for plasma sCSF1R in LCH

For patients receiving first-line therapy, plasma samples were collected at two time points: at the time of diagnosis and at week 6 (after the first initial induction therapy). For patients receiving dabrafenib treatment, serial blood samples were collected at every evaluation time point (baseline, one month, and every three months later) during follow-up. The levels of sCSF1R were tested using an automated microplate reader (Thermo, USA) at 450 nm according to the instructions of the Human CSF1R ELISA Kit (Boster, China).

Immunofluorescence staining of CSF1R in LCH lesions

Six biopsy samples from LCH patients at diagnosis were collected for immunofluorescence (IF) analysis. IF was performed as described. Briefly, tissue sections were deparaffinized, dehydrated, incubated with H₂O₂ for 20 minutes, subjected to high-pressure repair for 2 minutes, blocked with BSA for 30 minutes, and then incubated with anti-CSF1R and anti-*BRAF*-V600E antibodies at 4 °C overnight. The slices were incubated with the secondary antibody and evaluated via fluorescence microscopy.

Statistical analysis

All parameters were compared between patient groups by the χ^2 test, t test, one-way ANOVA, and *post hoc* Tukey's test according to the scale of the variable. For skewed data, a nonparametric test (Mann-Whitney U test) or one-way ANOVA and Tukey's test were applied after log transformation. To assess the correlation between sCSF1R and other parameters, Spearman's rank correlation coefficient (rS) was computed. Progression-free survival (PFS) was evaluated from the date of diagnosis until the date of one of the following events: progression, relapse, or death, whichever came first. PFS was estimated using the Kaplan–Meier method and compared with the log-rank test between subgroups. The prognostic value of plasma sCSF1R levels was studied using univariate and multivariate Cox models. All *P* values are shown as the results of two-sided tests. A *P* value < 0.05 was considered to indicate statistical significance. All the statistical analyses were performed by M Salama using SPSS software version 29.0 (SPSS, Inc., IL).

Results

Clinical characteristics of LCH patients

A total of 114 pediatric LCH patients with available plasma samples were enrolled in the present study. The patients' clinical characteristics are shown in Table 1. There were 70 boys and 44 girls in this study cohort. The median age at diagnosis was 4.46 years (range, 0.08 to 15.08 years). These included patients were classified as follows: 68 (59.6%) patients with SS LCH, 27 (23.7%) with MS RO- and 19 (16.7%) with MS RO+ LCH. There was no significant difference in clinical features between the 114 included patients and 25 excluded patients. The 114 studied LCH patients included 55 cases (48.2%) with *BRAF*-V600E mutation, 31 cases (27.2%) with *MAP2K1* mutation, 6 cases (5.3%) with *BRAF* indel mutation, 6 cases (5.3%) with *BRAF*-V600D mutation, 1 case (0.9%) with *ARAF* mutation, 1 case (0.9%) with c.1517+2.1517+3ins *BRAF* mutation and 14 cases (12.3%) without gene mutation.

Changes in the plasma proteome profile in LCH patients: identification of differentially expressed proteins

We explored the difference in plasma proteome profiles between 6 patients with MS RO+ LCH and 5 with SS LCH using DIA-based proteomic analysis. Nontargeted proteomics identified 85 DEPs in LCH plasma samples, 27 of which were upregulated and 58 of which were downregulated (fold change >1.5 and adjusted *P* < 0.05). Volcano plots (Figure 1A) and hierarchical clustering heatmaps (Figure 1B) illustrating the qualified and dysregulated proteins. The expression levels of the top nine up- and downregulated DEPs between the two classifications are shown in Supplementary Figure S1. GO analysis of the biological processes revealed enrichment of differentially expressed proteins involved in the acute-phase response and regulation of immune system processes (Figure 1C). KEGG analysis revealed that complement and coagulation cascades; pathways related to metabolism; and the PI3K-Akt, PPAR, MAPK, and NF-kappa B signaling pathways were significantly enriched (Figure 1D).

Identification of overlapping DEPs/DEGs by scRNA-seq versus plasma proteomics

We next performed a bioinformatics analysis of our previous scRNA-seq dataset from pediatric LCH PBMCs¹¹. We integrated 576 single cells from SS patients and 856 cells from MS RO+ patients to investigate the difference between the two disease extents. Nine cell clusters were identified by tSNE visualization (Figure 2A). We identified 322 differentially expressed genes (DEGs).

Furthermore, we identified three overlapping DEPs/DEGs, CSF1R, CD14, and GSN, between the scRNA-seq and plasma proteomics data (Figure 2B). The differential expression of the three DEGs in the single-cell

transcriptome of LCH PBMCs is shown in Figure 2C. Among the three candidates, CD14 is often considered a marker of classical monocyte cells, and GSN was found to be downregulated in the plasma of MS RO+ LCH patients. We focused on CSF1R for further analysis because it plays a critical role in the pathogenesis of LCH.

sCSF1R levels in plasma and CSF1R expression in LCH lesions

We determined plasma sCSF1R levels by ELISA to confirm the proteomic findings. The results showed that sCSF1R levels were greater in 104 LCH patients than in 10 healthy controls (median level: 38,823.8 vs. 18,172.6 pg/ml, $P < 0.001$; Figure 3A) and significantly differed among the three disease extents, with the most increased level occurring in the MS RO+ LCH group ($P < 0.001$; Figure 3B).

We further investigated the association between sCSF1R levels and the clinicopathological characteristics of LCH patients (Supplementary Figure S2). Patients younger than two years at diagnosis with skin, lung, or risk of organ involvement who were harboring the *BRAF*-V600E mutation in lesion tissues or cell-free DNA had increased sCSF1R. In addition, the plasma levels of several other DEPs were evaluated via ELISA in LCH patients (Supplementary Figure S3).

We analyzed the differential expression of CSF1R in LCH lesion cells by IF staining (Figure 3C). Consistently, patients with MS RO+ LCH had significantly greater CSF1R expression than did those with MS RO- LCH ($P < 0.01$) or SS-LCH ($P < 0.001$).

Prognostic significance of sCSF1R levels at diagnosis

ROC curve analysis revealed that plasma sCSF1R levels at diagnosis could efficiently predict the prognosis of pediatric LCH patients ($n=104$) treated with standard first-line treatment (AUC = 0.782, $P < 0.001$; Figure 4A), and an optimal cutoff for sCSF1R was chosen at 42,401.2 pg/ml by maximizing the Youden index. Using the cutoff values, we divided the whole cohort into high- and low-sCSF1R groups (72 and 32 patients, respectively). The 3-year PFS was significantly poorer in the high-sCSF1R subgroup than in the low-sCSF1R subgroup ($21.9\% \pm 7.3\%$ vs. $78.8\% \pm 4.9\%$, $P < 0.001$; Figure 4B). The prognostic impact of high-sCSF1R expression was significant in MS LCH patients ($P < 0.001$; Figure 4D) but not in SS-LCH patients ($P = 0.85$; Figure 4C).

Univariate analysis revealed that age at diagnosis; sex; bone, skin, liver, spleen, hematologic system, lung, pituitary, eye, ear, or lymph node involvement; and sCSF1R level were associated with the 3-year PFS of LCH patients (Figure 4E). Moreover, multivariate Cox proportional hazards regression analysis revealed that the sCSF1R concentration was an independent prognostic factor for 3-year PFS in children with LCH after we adjusted for these univariate risk factors (Figure 4F).

Monitoring sCSF1R levels during treatment

sCSF1R levels at week 6 of induction therapy were determined in 23 available plasma samples. After the 6-week course of initial induction treatment, ten patients were evaluated as active-disease (AD)-better, six patients were considered AD-stable, and seven patients developed progression and were evaluated as AD-worse. sCSF1R levels decreased significantly in the 16 patients who had AD-better/stable responses ($P < 0.0001$), whereas sCSF1R remained at high levels in those seven patients with disease progression (Figure 5A).

sCSF1R was sequentially monitored during dabrafenib treatment in thirteen MS LCH patients with the *BRAF*-V600E mutation (Supplementary Table S2). Six patients experienced relapse after discontinuation of dabrafenib (Figure 5B-G). The levels of sCSF1R obviously decreased after the initiation of dabrafenib administration but increased again at relapse, which was in accordance with the trend of cf*BRAF*-V600E. Notably, five (patients 1, 2, 4, 5 and 6) of the six patients had elevated sCSF1R levels 1-3 months before the clinical or radiographic appearance of recurrent lesions, which increased earlier than that of cf*BRAF*-V600E, indicating that sCSF1R levels provided a lead-time advantage over cf*BRAF*-V600E in predicting relapse (Figure 5B-G).

Of the seven patients who remained in remission, three had drug discontinuation (patients 7 to 9; Supplementary Figure S4A), and four had continuation (patients 10 to 13; Supplementary Figure S4B), and their sCSF1R levels were maintained at low levels during follow-up. Details of the longitudinal changes in sCSF1R and cf*BRAF* -V600E levels during dabrafenib treatment are shown in Supplementary Table S3.

sCSF1R increased the resistance of cells to the chemotherapeutic drug cytarabine

Transcriptome studies have shown that a few monocytes are potential precursors in the circulation for LCH^{11,12}. To evaluate the effect of sCSF1R on the chemosensitivity of LCH cells, we infected THP-1 cells with a *BRAF* -V600E overexpression lentivirus, which resulted in a significant increase in ERK1/2 phosphorylation (Supplementary Figure S5A). MTS experiments showed significantly elevated IC50 values after incubation with sCSF1R compared to those of the control (IC50: 4.6 vs . 2.3 $\mu\text{mol/L}$, $P = 0.02$; Supplementary Figure S5B), indicating increased resistance to cytarabine (Ara-C) resulting from sCSF1R treatment.

Discussion

Liquid biopsy provides enhanced sensitivity for biomarker discovery and ease of repeated sampling throughout treatment in a much more convenient and noninvasive way^{13,14}. Recent advances in mass spectrometry (MS)-based proteomics have greatly extended its reach in biomedical and clinical research, and mass spectrometry (MS) is now poised to characterize the plasma proteome in great depth¹⁵. Plasma proteomic analysis has proven to be a promising tool for identifying new and effective biomarkers that can be used for evaluating the prognosis and treatment response in patients with various cancers¹⁶.

Patients with RO+ LCH have a poorer prognosis than patients with RO-LCH¹⁷. Recent evidence from the myeloid dendritic cell (DC) model suggested that MS-RO+ LCH results from a driver mutation in a bone marrow (BM)-resident multipotent hematopoietic progenitor¹⁸. However, the exact mechanism is unknown. Herein, we focused on the differences in plasma proteome profiles between RO+ LCH patients and SS LCH patients, and our study is the first, to our knowledge, to identify a novel soluble form of CSF1R in the plasma of pediatric LCH patients.

The results of the ELISA validation showed that plasma sCSF1R levels were associated with disease extent, and high levels of sCSF1R correlated with more severe disease, as indicated by a younger age; involvement of the RO, skin, and lung; and the presence of the *BRAF*-V600E mutation in lesions or cfDNA. Moreover, a high sCSF1R level at diagnosis independently predicted inferior PFS and was sustained in patients who experienced disease progression after 6 weeks of treatment. Notably, dynamic monitoring of sCSF1R levels provided an early warning of relapse in patients receiving *BRAF* inhibitor treatment. Therefore, the sCSF1R level should be closely monitored, especially during treatment with targeted inhibitors of *BRAF* or other proteins in the MAPK pathway.

IF staining in this study showed that high CSF1R protein expression in LCH lesions was associated with RO involvement, which was in line with the plasma sCSF1R levels. We also noted that sCSF1R levels apparently decreased after dabrafenib administration initiation, suggesting that extracellular CSF1R in plasma was mainly secreted by cells that carried the *BRAF* -V600E driver mutation. In vitro drug sensitivity data showed that sCSF1R increased resistance to Ara-C in THP-1 cells expressing ectopic *BRAF* -V600E. However, the exact biological function of sCSF1R is unclear. The release of soluble forms may represent a mechanism for counter regulation of CSF1R. A recent study revealed that overexpression of sCSF1R significantly decreased the extent of microgliosis in both the dorsal and ventral horns, indicating that sCSF1R can reduce the activation of native CSF1R on microglia¹⁹. By acting as a decoy receptor, sCSF1R can bind to colony-stimulating Factor 1 (CSF1) and prevent it from interacting with the membrane-bound CSF1R on target cells, possibly modulating CSF1 signaling and affecting the recruitment, survival, and differentiation of cells. In contrast, our data showed that sCSF1R was closely linked to severe disease and relapse in LCH patients, suggesting that sCSF1R contributes to disease progression. Previous studies have suggested that several oxidative stress proteins, including thioredoxin and heat shock proteins, are released from stressed, transformed cells and act as “endogenous” danger signals by binding TLR4 in the extracellular microenvironment, which results in the activation of downstream pathways and the secretion of

proinflammatory cytokines^{20,21}. We thus speculated that sCSF1R may act as an endogenous danger signal by binding to danger signal sensors/receptors, which is independent of CSF1. However, further investigations are needed to explore the underlying mechanisms involved.

Several recent studies have shown the good short-term effectiveness and tolerability of BRAF or MEK inhibitors in recurrent/refractory LCH²²⁻²⁵. However, MAPK pathway inhibition did not appear to be curative and was associated with a high risk of reactivation following drug discontinuation²⁶⁻²⁸. Pharmacological inhibition of CSF1R has emerged as a promising antitumor strategy, and several small-molecule CSF1R inhibitors have been developed in clinical and preclinical studies²⁹. Thus, combined inhibition of BRAF/MAPK signaling and CSF1R may be beneficial for recurrent/refractory LCH treatment. However, most clinical results on the safety and efficacy of CSF1R inhibition are limited³⁰, which may be caused, in part, by a high level of plasma sCSF1R, as shown in this study. Therefore, monoclonal antibodies engineered to recognize the extracellular domains of CSF1R may inspire new ideas for recurrent/refractory LCH treatment.

One limitation of this study was the lack of a validation cohort for the prognostic analyses of sCSF1R. Additional studies in independent cohorts are needed to establish the validity of our findings.

In conclusion, our findings identify plasma sCSF1R as a promising prognostic indicator for pediatric LCH. Accurate measurements of plasma sCSF1R at diagnosis and during follow-up have potential academic and clinical importance, and exploring such effective biomarkers to facilitate risk stratification and precision medicine is the major challenge for LCH treatment.

References

1. Allen CE, Merad M, McClain KL. Langerhans-Cell Histiocytosis. *N Engl J Med* . Aug 30 2018;379(9):856-868. doi:10.1056/NEJMra1607548
2. McClain KL, Bigenwald C, Collin M, et al. Histiocytic disorders. *Nat Rev Dis Primers* . Oct 7 2021;7(1):73. doi:10.1038/s41572-021-00307-9
3. Krooks J, Minkov M, Weatherall AG. Langerhans cell histiocytosis in children: History, classification, pathobiology, clinical manifestations, and prognosis. *J Am Acad Dermatol* . Jun 2018;78(6):1035-1044. doi:10.1016/j.jaad.2017.05.059
4. Xiang C, Li H, Tang W. Targeting CSF-1R represents an effective strategy in modulating inflammatory diseases. *Pharmacol Res* . Jan 2023;187:106566. doi:10.1016/j.phrs.2022.106566
5. Hagan N, Kane JL, Grover D, et al. CSF1R signaling is a regulator of pathogenesis in progressive MS. *Cell Death Dis* . Oct 23 2020;11(10):904. doi:10.1038/s41419-020-03084-7
6. Ozkaya N, Lee I, Johnson TS, Jaffe ES. CSF1R/CD115 is a Helpful Marker for the Distinction of Florid Dermatopathic Lymphadenopathy From Langerhans Cell Neoplasms. *Am J Surg Pathol* . Jul 1 2023;47(7):844-846. doi:10.1097/pas.0000000000002047
7. Lonardi S, Scutera S, Licini S, et al. CSF1R Is Required for Differentiation and Migration of Langerhans Cells and Langerhans Cell Histiocytosis. *Cancer Immunol Res* . Jun 2020;8(6):829-841. doi:10.1158/2326-6066.Cir-19-0232
8. Barreda DR, Hanington PC, Stafford JL, Belosevic M. A novel soluble form of the CSF-1 receptor inhibits proliferation of self-renewing macrophages of goldfish (*Carassius auratus* L.). *Dev Comp Immunol* . 2005;29(10):879-94. doi:10.1016/j.dci.2005.02.006
9. Shi M, Movius J, Dator R, et al. Cerebrospinal fluid peptides as potential Parkinson disease biomarkers: a staged pipeline for discovery and validation. *Mol Cell Proteomics* . Mar 2015;14(3):544-55. doi:10.1074/mcp.M114.040576

10. Cui L, Zhang L, Ma HH, et al. Circulating cell-free BRAF V600E during chemotherapy is associated with prognosis of children with Langerhans cell histiocytosis. *Haematologica* . Sep 1 2020;105(9):e444-447. doi:10.3324/haematol.2019.229187
11. Shi H, He H, Cui L, et al. Transcriptomic landscape of circulating mononuclear phagocytes in Langerhans cell histiocytosis at the single-cell level. *Blood* . Oct 7 2021;138(14):1237-1248. doi:10.1182/blood.2020009064
12. Schwentner R, Jug G, Kauer MO, et al. JAG2 signaling induces differentiation of CD14(+) monocytes into Langerhans cell histiocytosis-like cells. *J Leukoc Biol* . Jan 2019;105(1):101-111. doi:10.1002/jlb.1a0318-098r
13. Lone SN, Nisar S, Masoodi T, et al. Liquid biopsy: a step closer to transform diagnosis, prognosis and future of cancer treatments. *Mol Cancer* . Mar 18 2022;21(1):79. doi:10.1186/s12943-022-01543-7
14. Ding Z, Wang N, Ji N, Chen ZS. Proteomics technologies for cancer liquid biopsies. *Mol Cancer* . Feb 15 2022;21(1):53. doi:10.1186/s12943-022-01526-8
15. Budayeva HG, Kirkpatrick DS. Monitoring protein communities and their responses to therapeutics. *Nat Rev Drug Discov* . Jun 2020;19(6):414-426. doi:10.1038/s41573-020-0063-y
16. Murakami I, Oh Y, Morimoto A, et al. Acute-phase ITIH4 levels distinguish multi-system from single-system Langerhans cell histiocytosis via plasma peptidomics. *Clin Proteomics* . 2015;12(1):16. doi:10.1186/s12014-015-9089-2
17. Cui L, Wang CJ, Lian HY, et al. Clinical outcomes and prognostic risk factors of Langerhans cell histiocytosis in children: Results from the BCH-LCH 2014 protocol study. *Am J Hematol* . Apr 2023;98(4):598-607. doi:10.1002/ajh.26829
18. Xiao Y, van Halteren AGS, Lei X, et al. Bone marrow-derived myeloid progenitors as driver mutation carriers in high- and low-risk Langerhans cell histiocytosis. *Blood* . Nov 5 2020;136(19):2188-2199. doi:10.1182/blood.2020005209
19. Gushchina S, Yip PK, Parry GA, et al. Alleviation of neuropathic pain by over-expressing a soluble colony-stimulating factor 1 receptor to suppress microgliosis and macrophage accumulation. *Glia* . Dec 2021;69(12):2963-2980. doi:10.1002/glia.24085
20. Riddell JR, Wang XY, Minderman H, Gollnick SO. Peroxiredoxin 1 stimulates secretion of proinflammatory cytokines by binding to TLR4. *J Immunol* . Jan 15 2010;184(2):1022-30. doi:10.4049/jimmunol.0901945
21. Asea A, Rehli M, Kabingu E, et al. Novel signal transduction pathway utilized by extracellular HSP70: role of toll-like receptor (TLR) 2 and TLR4. *J Biol Chem* . Apr 26 2002;277(17):15028-34. doi:10.1074/jbc.M200497200
22. Diamond EL, Subbiah V, Lockhart AC, et al. Vemurafenib for BRAF V600-Mutant Erdheim-Chester Disease and Langerhans Cell Histiocytosis: Analysis of Data From the Histology-Independent, Phase 2, Open-label VE-BASKET Study. *JAMA Oncol* . Mar 1 2018;4(3):384-388. doi:10.1001/jamaoncol.2017.5029
23. Kieran MW, Geoerger B, Dunkel IJ, et al. A Phase I and Pharmacokinetic Study of Oral Dabrafenib in Children and Adolescent Patients with Recurrent or Refractory BRAF V600 Mutation-Positive Solid Tumors. *Clin Cancer Res* . Dec 15 2019;25(24):7294-7302. doi:10.1158/1078-0432.Ccr-17-3572
24. Wang D, Chen XH, Wei A, et al. Clinical features and treatment outcomes of pediatric Langerhans cell histiocytosis with macrophage activation syndrome-hemophagocytic lymphohistiocytosis. *Orphanet J Rare Dis* . Apr 4 2022;17(1):151. doi:10.1186/s13023-022-02276-y
25. Kolenová A, Schwentner R, Jug G, et al. Targeted inhibition of the MAPK pathway: emerging salvage option for progressive life-threatening multisystem LCH. *Blood Adv* . Feb 14 2017;1(6):352-356. doi:10.1182/bloodadvances.2016003533

26. Gulati N, Allen CE. Langerhans cell histiocytosis: Version 2021. *Hematol Oncol* . Jun 2021;39 Suppl 1(Suppl 1):15-23. doi:10.1002/hon.2857
27. Donadieu J, Larabi IA, Tardieu M, et al. Vemurafenib for Refractory Multisystem Langerhans Cell Histiocytosis in Children: An International Observational Study. *J Clin Oncol* . Nov 1 2019;37(31):2857-2865. doi:10.1200/jco.19.00456
28. Eckstein OS, Visser J, Rodriguez-Galindo C, Allen CE. Clinical responses and persistent BRAF V600E(+) blood cells in children with LCH treated with MAPK pathway inhibition. *Blood* . Apr 11 2019;133(15):1691-1694. doi:10.1182/blood-2018-10-878363
29. Wen J, Wang S, Guo R, Liu D. CSF1R inhibitors are emerging immunotherapeutic drugs for cancer treatment. *Eur J Med Chem* . Jan 5 2023;245(Pt 1):114884. doi:10.1016/j.ejmech.2022.114884
30. Cannarile MA, Weisser M, Jacob W, Jegg AM, Ries CH, Rüttinger D. Colony-stimulating factor 1 receptor (CSF1R) inhibitors in cancer therapy. *J Immunother Cancer* . Jul 18 2017;5(1):53. doi:10.1186/s40425-017-0257-y

Figure legends

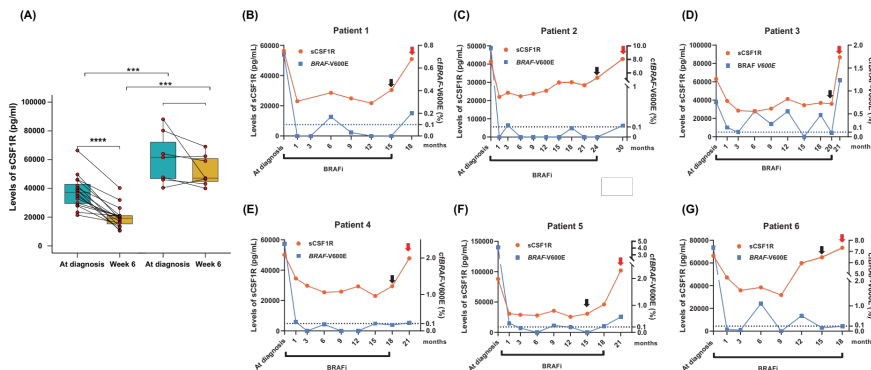
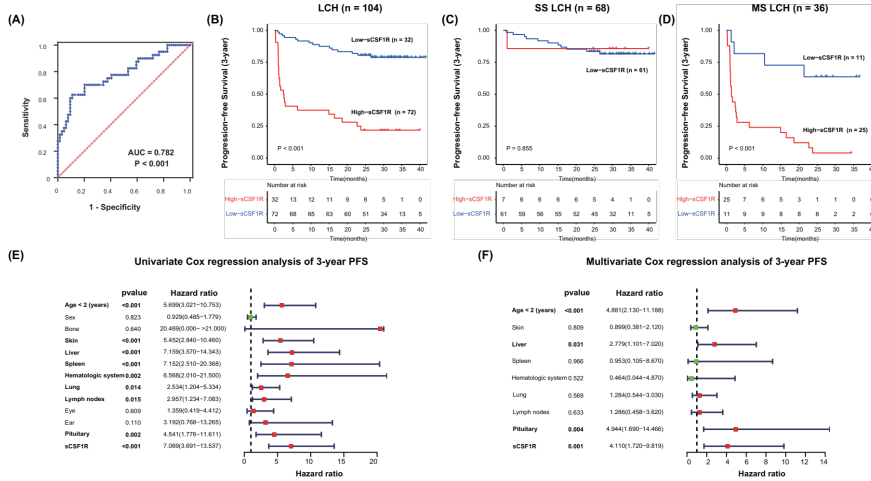
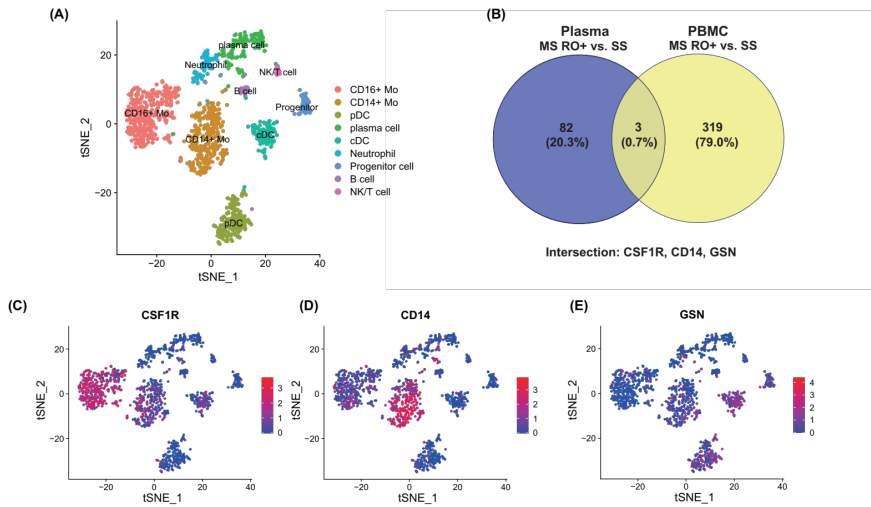
Figure 1. DEP screening and annotation enrichment analysis of the plasma proteome profiles of pediatric LCH patients. (A) Volcano plot of DEPs between the MS LCH and SS LCH groups. The blue points represent downregulated proteins, while the red points represent upregulated proteins. (B) Hierarchical clustering heatmap of the screened DEPs. (C) KEGG annotation and enrichment analysis of DEPs showing the signaling pathway diagram for the enriched items. (D) Gene Ontology annotation and enrichment analysis of DEPs, including biological process (BP), molecular function (MF), and cellular component (CC) terms.

Figure 2. Identification of overlapping DEPs/DEGs by scRNA-seq versus plasma proteomics. (A) T-distributed stochastic neighbor embedding (t-SNE) plot of nine PBMC subclusters from MS RO+ LCH (n= 7) and SS LCH (n=3) patients. (B) Venn diagram illustrating the intersections between the two comparisons according to plasma proteomics versus scRNA-seq. (C) The feature plot shows the clustering of common DEGs (*CSF1R* , *CD14* , and *GSN*) based on gene expression. The color legend shows the log₁₀-transformed expression levels of the genes.

Figure 3. sCSF1R levels in plasma and CSF1R expression in LCH lesions. (A) sCSF1R levels in plasma samples from LCH patients and healthy children determined by ELISA. (B) Scatter plots showing the differences in sCSF1R levels among SS, MS RO-, and MS RO+ LCH patients. (C) Representative images of immunofluorescence staining for *BRAF*- V600E (pink) and CSF1R (green) in LCH skin biopsies. Original magnification: 100×; scale bar: 50 μm. Histogram of MFI (average fluorescence intensity) among SS, MS RO-, and MS RO+ LCH.

Figure 4. Prognostic value of plasma sCSF1R levels at diagnosis. (A) ROC curve schematic. (B) 3-year PFS in the cohort of 104 LCH patients treated with standard first-line treatment. (C) PFS in patients with SS LCH (n= 68). (D) 3-year PFS in patients with MS LCH (n= 36). (E-F) Univariate and multivariate analyses of prognostic factors for PFS in children with LCH.

Figure 5. Monitoring of plasma sCSF1R levels during follow-up in LCH patients. (A) The levels of plasma sCSF1R at two time points (at diagnosis and at week 6) in 23 patients receiving first-line therapy. (B-G) Dynamics of the plasma sCSF1R and *cfBRAF* -V600E levels in six relapsed patients treated with BRAFi therapy. The black arrows indicate the time points at which patients stopped treatment with darafenib; the red arrows indicate the time of recurrence. Treatment regimens are indicated at the bottom of each graph. The limit of the *cfBRAF* -V600E detection assay was determined to be 0.1%.



Hosted file

Table 1-0125.docx available at <https://authorea.com/users/333532/articles/723194-the-plasma-soluble-csf1r-level-is-a-promising-prognostic-indicator-for-pediatric-langerhans-cell-histiocytosis>